


Advances in high-throughput crop phenotyping using unmanned aerial vehicles (UAVs)

Book Chapter**Author(s):**

Aasen, Helge; Roth, Lukas 

Publication date:

2022

Permanent link:

<https://doi.org/10.3929/ethz-b-000560485>

Rights / license:

[In Copyright - Non-Commercial Use Permitted](#)

Originally published in:

<https://doi.org/10.19103/as.2022.0102.09>

Funding acknowledgement:

198091 - PhenomEn (SNF)

195591 - Canopy temperature dynamics as proxy for photosynthetic induction (SNF)

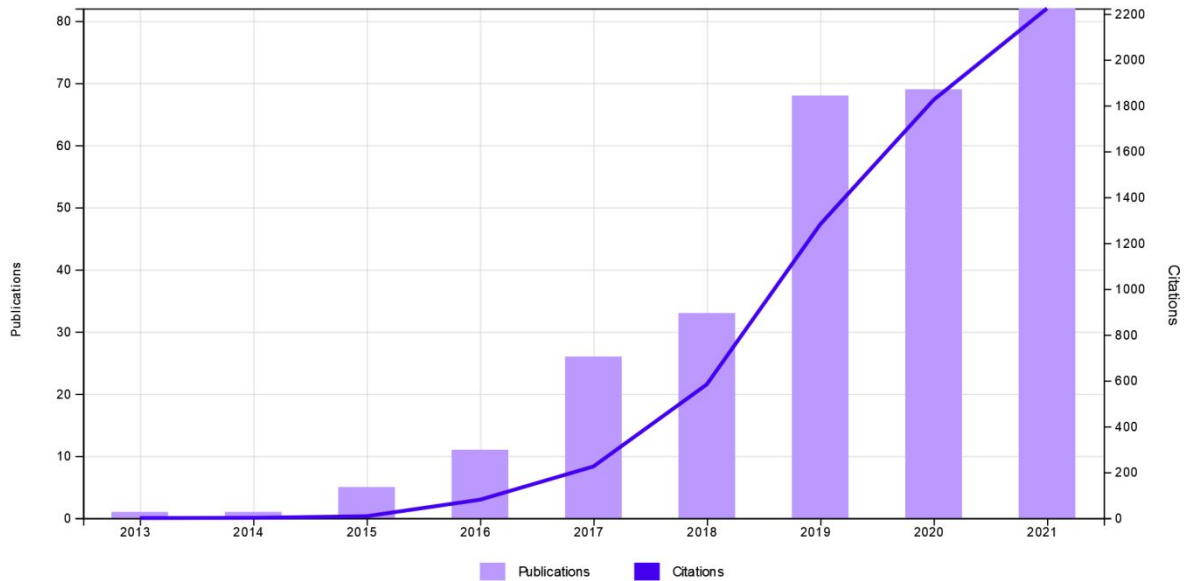
172433 - Reconciling innovative farming practices and networks to enable sustainable development of smart Swiss farming systems (SNF)

Remote sensing on the plant scientists' playground – recent trends and future perspectives for high- throughput field phenotyping with UAVs

1. Introduction

Many scientific disciplines use UAVs (Aasen et al., 2018; Adão et al., 2017; Colomina and Molina, 2014; Maes and Steppe, 2019; Pádua et al., 2017; Pajares, 2015, 2015; Sanchez-Azofeifa et al., 2017; Warner and Cracknell, 2017; Zarco-Tejada, 2008; Zhang and Kovacs, 2012) and some have even said they revolutionize disciplines (Anderson and Gaston, 2013; McCabe et al., 2017; Sanchez-Azofeifa et al., 2017). Already more than 10 years ago, unmanned aerial vehicles (UAVs) were envisioned to bring about a new era in Agriculture (Zarco-Tejada, 2008). Seen from today's perspective, the biggest impact can be seen in the application of UAVs in high-throughput field phenotyping. Field phenotyping refers to a quantitative description of a plant's phenotype - i.e. its anatomical, ontogenetical, physiological, and biochemical properties - in its natural environment (Walter et al., 2015). In the context of breeding, where hundreds or even thousands of different genotypes need to be screened for their performance, high-throughput field phenotyping allows the timely and rapid screening of multiple traits in early breeding stages, with the potential to reduce the duration of breeding cycles and avoid loss of potentially important alleles due to linkage drag (Araus and Cairns, 2014; Furbank and Tester, 2011; Rebetzke et al., 2019).

Since UAV sensing systems have matured as remote sensing platforms (Aasen et al., 2018), almost all "big players" (research groups, companies, organizations, ...) in the area of field phenotyping have started to use UAVs for their measurements (see reviews of (Araus et al., 2018; Cendrero-Mateo et al., 2017; Hund et al., 2019a; Rebetzke et al., 2019; Tardieu et al., 2017)). This has led to an adaption of remote sensing technologies by agronomists, which is also reflected by an exponential increase of publications (Figure 2) and have greatly helped to relieve the phenotyping bottleneck.



28

29 *Figure 1 Number of publications and citations with the topics field phenotyping and UAVs¹*

30 This trend can be seen as a welcomed development, since the large toolbox of remote sensing has long
 31 been underexplored in agricultural sciences. Unfortunately, applying UAV technologies also comes
 32 with some hurdles, since not every agronomist embarking on that journey has a background in remote
 33 sensing or image processing. Additionally, some have been deceived by promises put forward by the
 34 marketing of companies shading the challenges that one has to face from the step of being able to fly
 35 a certain sensor to reliable trait extraction. In the following we will reflect on UAV remote sensing
 36 along with data analysis approaches in the toolbox for high-throughput field phenotyping and
 37 ecophysiological research.

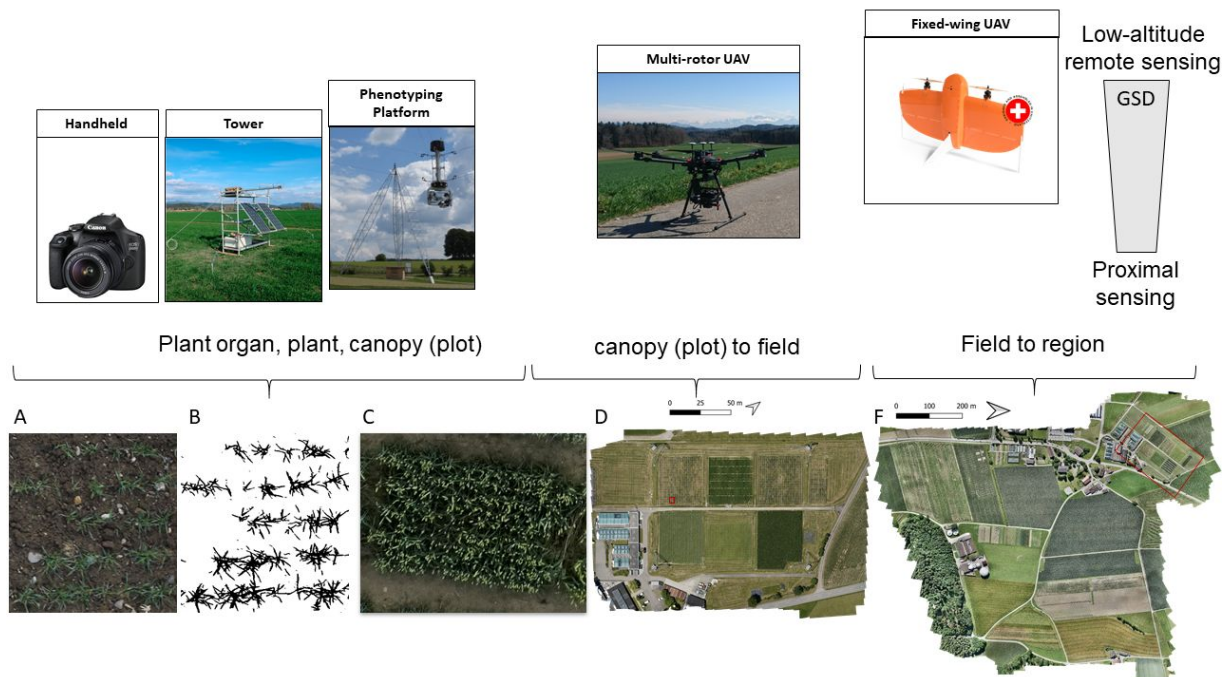
38 **2. Remote sensing tools for the plant scientists' playground**

39 **2.1. UAVs**

40 In a typical field phenotyping scenario, a couple of hundred to thousand plots (patches of crop canopies
 41 with uniform conditions, ranging in size from single plants/rows to machine harvestable yield plots of
 42 a few meters) situated on a few hectares need to be screened. UAV remote sensing combines the
 43 potential of capturing highly spatially resolved data with high throughput and a great choice of sensors.
 44 On the other extreme to UAVs, handheld measurements have a very attractive setup cost, are easy to
 45 setup and are highly flexible (Aasen et al., 2020; Perich et al., 2020). Along with phenotyping stations

¹ ts=((UAV* or UAS* or "unmanned aerial vehicle*" or "unmanned aerial system*" or "unmanned aircraft system*" or "RPAS" or "remotely piloted aircraft system") and (phenotyping or "field phenotyping" or "field-phenotyping")) and Articles or Review Articles or Early Access (Document Types) and Articles or Review Articles or Book Chapters (Document Types)

46 such as the ‘Field Phenotyping Platform’ (FIP) at ETH Zürich (Kirchgessner et al., 2017), the ‘Field
 47 Scanalyzer’ in Rothamsted (Virlet et al., 2017) and similar stations described in (Hund et al., 2019b),
 48 handheld measurements arguably have the highest GSDs available. However, sampling large field
 49 experiments with such devices is in most cases unfeasible due to the high running costs and the long
 50 time needed to sample a whole experiment with potentially hundreds of plots: Changes in
 51 environmental conditions during the sample time might bias the results, i.e., in case of thermal and
 52 spectral measurements (Deery et al., 2016a; Perich et al., 2020; Sagan et al., 2019).



53

54 *Figure 2 UAVs sensing systems in comparison with other field phenotyping approaches regarding*
 55 *coverage and ground sampling distance (GSD). A and B are a image taken with the Field Phenotyping*
 56 *Platform (FIP) with 0.0005 m GSD and a segmentation of leaves using the method of (Zenkl et al., “in*
 57 *review”). C is the area of a plot extracted from a multi-rotor UAV flying at 30 m AGA with 0.003 m GSD.*
 58 *D is an orthomosaic with an extend of 2 ha and a GSD of 0.008 m generated from a multi-rotor UAV*
 59 *flying at 80 m above ground altitude (AGA). The red rectangle marks the area of C. E is an orthomosaic*
 60 *with an extend of approximately 60 ha and a GSD of 0.013 m generated from with a fixed-wing UAV*
 61 *flown at 110 m AGA. The red rectangle marks the area of D.*

62 In contrast to phenotyping stations, UAVs have the advantage of low setup and running costs of the
 63 measurement system. Additionally, the size of the coverable area is only limited by the flight time of
 64 the carrier system but can be extended by combining imagery from multiple flights (Perich et al., 2020)
 65 or by adjusting the flight height by the cost of lowering the ground sampling distance (GSD). While
 66 multi-rotor systems are more flexible when it comes to flight trajectory, fixed wing UAVs are more
 67 efficient when it comes to areal coverage. Besides, multi-rotor UAVs have greater payload potential
 68 than fixed wing UAVs. The latter allows to mount a wide range of spectral, thermal, RGB or LiDAR
 69 sensors (Aasen et al., 2018; Lucieer et al., “in preparation”; Yang et al., 2017).

70 Overall, UAVs can measure traits of interest with relatively little effort across several ha in a couple of
71 minutes. The exact coverage per time depends on the ground sampling distance necessary to extract
72 the trait of interest. Additionally, due to the low manual effort, measures can be carried out in a high
73 temporal frequency, with no disturbance of the soil or plants, and potentially by non-experts, since the
74 flight path and data capturing procedure can be programmed. Finally, UAVs allow to carry out the same
75 measurements at multiple places. However, key to a repeatable and reliable trait extraction are well
76 established flight (c.f. subsection 2.2) and trait extraction protocols (c.f. section 3).

77 **2.2. Flight protocols**

78 Defining UAV measurement protocols can be complex. It requires good knowledge and experience not
79 only about the sensing system, but also about the data processing workflow and the analysis methods
80 (Aasen et al., 2018). Moreover, to harvest the full potential and reduce the effort for each flight, the
81 area of interest should be equipped with auxiliary infrastructure such as georeferencing ground control
82 points (GCPs) or radiometric ground control points (RCPs). Finally, the flight plan and sensing
83 equipment (flight height, flight speed, angular composition of the data, focal length, image resolution,
84 exposure time) need to match the requirements given for the trait of interest (ground sampling
85 distance and motion blur). Luckily, several tools are available to help with configuring the flight
86 parameters and equipping area of interest (Roth et al., 2018b).

87 **3. A flight through major plant traits that can be extracted with UAV** 88 **remote sensing**

89 In the following, we will go through some important traits for field phenotyping. The objective of this
90 chapter is to align the definitions of the agronomic community with terminology of the remote sensing
91 community and give hints of where remote sensing methods could be used in the context of field
92 phenotyping. Then, some examples approaches are highlighted.

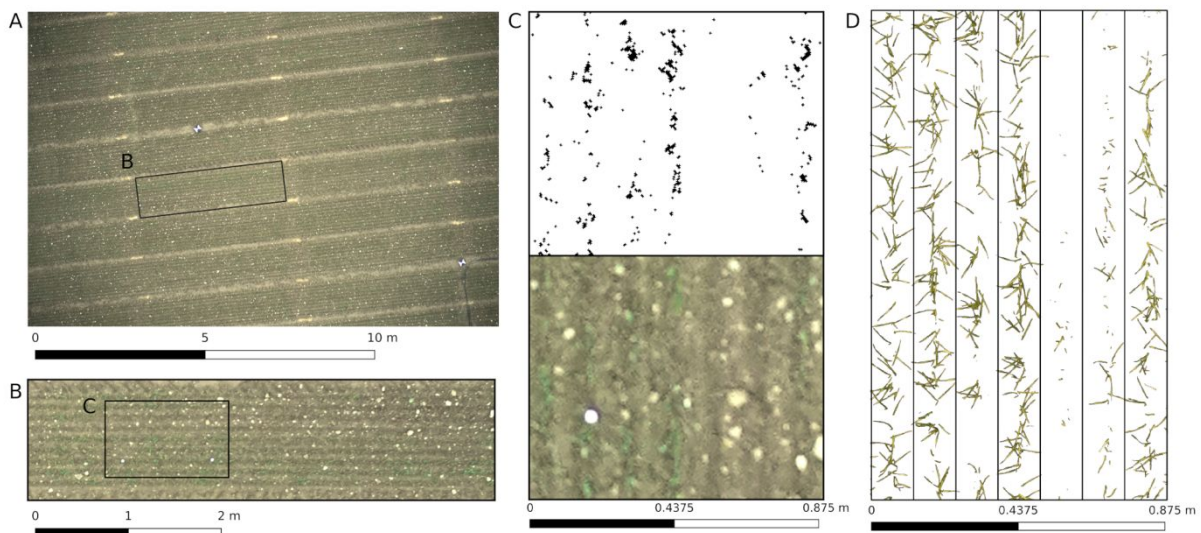
93 **3.1. Canopy cover and leaf area index**

94 Different terms exist to describe the foliage of plant canopies. While the canopy cover describes how
95 well a plant canopy covers the soil, a physiologically more relevant term is the leaf area index (LAI) that
96 describes the total leaf area per ground area. The LAI can reach up to values far above one (e.g., around
97 six for wheat at the end of the vegetative stage) if multiple layers of leaves in a canopy cover a ground
98 area. Unfortunately, it is challenging to measure the LAI nondestructively as soon as multiple leaf layers
99 overlap. Even in the early season where overlaps are sparse it is not straight forward to estimate LAI:
100 Leaves are often not planar and growth at a certain inclination angle, leading to a complex 3D
101 geometry, which makes it difficult to estimate a correct leaf area, and oblique viewing geometries (e.g.,

102 towards the edge of an image) may introduce biases due to perspective distortion². Keeping these
103 constrains in mind, two major approaches are used to estimate the leaf area, namely i) image-based
104 leaf from soil segmentation and ii) absorption-based proxy measurements.

105 3.1.1. Leaf area estimation by image segmentation

106 Image segmentation-based leaf area estimation is based on the differentiation of “green” leaf pixels
107 and “brown” soil pixels by some kind of classification. Then, the apparent ratio of “green” to total pixels
108 is expressed as the canopy cover. Sometimes, the resulting quantities are also referred to as fractional
109 cover or green cover. Besides of the constrains mentioned above, the precision of this method relies
110 on the possibility to differentiate “green” from “brown” pixels on the image. Consequently, the ground
111 sampling distance and motion blur need to be tuned such that the necessary precision can be reached
112 (Hu et al., 2019; Roth et al., 2018b) – which is relative to the organ (leaf) size and thus, crop specific
113 (c.f. Figure 3). Moreover, shadows and overexposure of reflecting leaf parts might compromise the
114 precision of classification.



115

116 *Figure 3: Example of UAV image of wheat (A, B, C) with a ground sampling distance of 3 mm per pixel*
117 *that covers an area of approximately 13 x 9 m in comparison to an image captured with the field*
118 *phenotyping platform (FIP) of ETH Zurich with a ground sampling distance of 0.3 mm per pixel that*
119 *covers an area of approximately 0.9 x 1.2 m (D), both taken at 2018-11-12 a month after sowing.*
120 *Illustrated are the original RGB images (A), the shape of the yield plot (B), a subsample of the plot where*
121 *a random forest segmentation approach was applied (Roth et al., 2020) (C) and the same subsample*
122 *in a FIP image where a deep learning semantic segmentation was applied (Zenkl et al., “in review”) (D).*

123 Today decision tree based segmentation (e.g. Random Forest) classifiers (in their simplest form as an
124 Otsu thresholding, e.g. (Torres-Sánchez et al., 2014)), often in combination with different color space
125 transformations to make the classification more robust (Roth et al., 2020, 2018a) are often used to

² The curious reader may grab his/her rubber boots, go to a crop field and look at the same spot from right above the spot and a few meters aside from it.

126 segment “green” from “brown”. The most recent segmentation approaches also include the
127 information of neighboring pixels for the classification. A recent study by Zenkle et al. (“in review”)
128 compared different segmentation approaches for very-high resolution RGB images (0.003 m) of the
129 “*Eschikon Wheat Segmentation Dataset*” (Zenkl et al., “in review”) and concluded that a deep learning
130 based approach outperformed other machine learning methods which use Support Vector Machines
131 and/or Random Forrest. Most methods are able to assign uncertainties to the prediction (Figure 2),
132 which allows carrying-forward these uncertainties to subsequent processing steps. However, to
133 perform such studies, well annotated datasets such as the “*Eschikon Wheat Segmentation Dataset*”
134 (Zenkl et al., “in review”) are necessary (c.f. other chapter). The last “trick” to be mentioned for leaf
135 area estimation by image segmentation is to use the full information of multiple overlapping images
136 captured from different angles. This so called “multiview imaging” combines the complementary
137 information included in these images to improve the prediction of leaf area (Roth et al., 2020, 2018a).
138 Still, all segmentation-based methods reach their limit as soon as full canopy closure is reached.

139 **3.1.2. Absorption based leaf area estimation**

140 A different approach is to use the absorption of plant matter (respectively the change in reflection
141 from a surface covered by vegetation) to approximate the plant material in an area of interest. This
142 approach is particularly useful when the ground sampling distance is not sufficient to discriminate
143 plants from soil background.

144 Consequently, this approach has a long history in remote sensing. Several methods and algorithms can
145 be used to generate models for plant trait retrieval from spectral data. Parametric regression methods,
146 such as vegetation indices (VIs, the most well-known one being the normalized difference vegetation
147 index (NDVI; (Rouse, Jr. et al., 1974)) combine information from several wavelength bands. Linear
148 nonparametric regression methods (sometimes called chemometric techniques (Atzberger et al.,
149 2010)), such as principle component analysis and partial least squares regression, take into account
150 the full spectrum. More recently, nonlinear nonparametric methods, often referred to as machine
151 learning regression algorithms (MLRAs), are increasingly being applied in remote sensing. Examples
152 include decision trees (e.g. random forest), artificial neural networks and kernel-based regression (e.g.
153 Gaussian process regression) methods. Their main advantage is that they can capture nonlinear
154 relationships without needing to know the underlying data distribution, and hence without assuming
155 a particular probability density distribution. Thus they are perfectly suited to spectroscopic data and
156 have been shown to outperform other methods (for more detailed information please refer to the
157 reviews of Verrelst et al., 2019, 2015).

158 The general advantage of spectral data-based approaches is, that they can increase the throughput
159 significantly since absorption-based approximation of plant traits are not depending on very-high

160 ground sampling distances to segment objects. Consequently, they allow to fly higher and faster. Also,
161 they can discriminate the amount of plant matter even when multiple layers of leaves overlap. The
162 disadvantage however is that if absolute values from one day to another or one field to another are to
163 be compared, radiometrically and spectrally calibrated devices should be used (for a review on the
164 current state of the art in UAV spectral remote sensing please refer to (Aasen et al., 2018)). When only
165 relative differences at one location are needed, uncalibrated systems may also be suitable as long as
166 the image capturing settings and conditions remain constant (Rasmussen et al., 2016).

167 Besides, structural properties of the canopy such as leaf angle have an impact on the apparent spectral
168 reflectance of a canopy and may bias the retrieval of plant traits (Wan et al., 2021; e.g. Zou et al., 2018;
169 Zou and Möttus, 2015). Consequently, empirical relationship of spectral reflectance indices and plant
170 traits are not always stable across years and phenological stages (Aasen et al., 2014; Gnyp et al., 2013).
171 To the authors knowledge, the robustness across different genotypes has not yet been assessed. Still,
172 one may also exercise caution when using empirical models for plant trait retrieval from spectral data
173 – in particular in the context of breeding, where structural properties of new varieties are unknown.
174 Inverting physically based radiative transfer model may be a way forward, since it builds on
175 mechanical relationships between the spectral formation and biophysical and structural plant traits
176 (Verrelst et al., 2015).

177 **3.2. Plant emergence, density and tillering**

178 Important drivers of yield are the number of shoots that bear harvestable organs. This number is
179 determined by two parameters: (1) The number of plants per area (which itself is the product of the
180 sowing density and germination rate), and (2) by the branching rate (often called tillering rate).
181 Estimating the number of plants per area as well as the number of tillers per area allows determining
182 the germination rate, the tillering rate, and related dynamics' parameters. Consequently,
183 corresponding high-throughput approaches are of high interest for UAV based field phenotyping.

184 Monitoring the development of plants and tillers is usually done early in the season when canopies
185 establish. Two types of approaches have been assessed for this early growth phase, namely coverage-
186 based approaches and counting approaches. Coverage based approaches use some kind of metric to
187 assess the greenness within an area of interest and are therefore closely related to canopy cover and
188 leaf area approaches (c.f. section 2.2). Consequently, they measure the totality of the canopy and are
189 unable to distinguish tillers from main shoots. Therefore, they can only estimate number of tillers and
190 not number of plants (Phillips et al., 2004; Scotford and Miller, 2004). In addition, coverage-based
191 estimation approaches are based on empirically determined parameters and may therefore be biased
192 by genotype and environment specific variances that are unrelated to the tiller density. On the positive
193 side, coverage-based approaches demand for a relatively low ground sampling distance. To overcome

194 the limitations of pure coverage-based approaches while still working with low ground sampling
195 distances, Roth et al. (2020) used a multi-view approach to harvest the information contained in
196 multiple overlapping images to improve the prediction of plant and tiller count estimation.

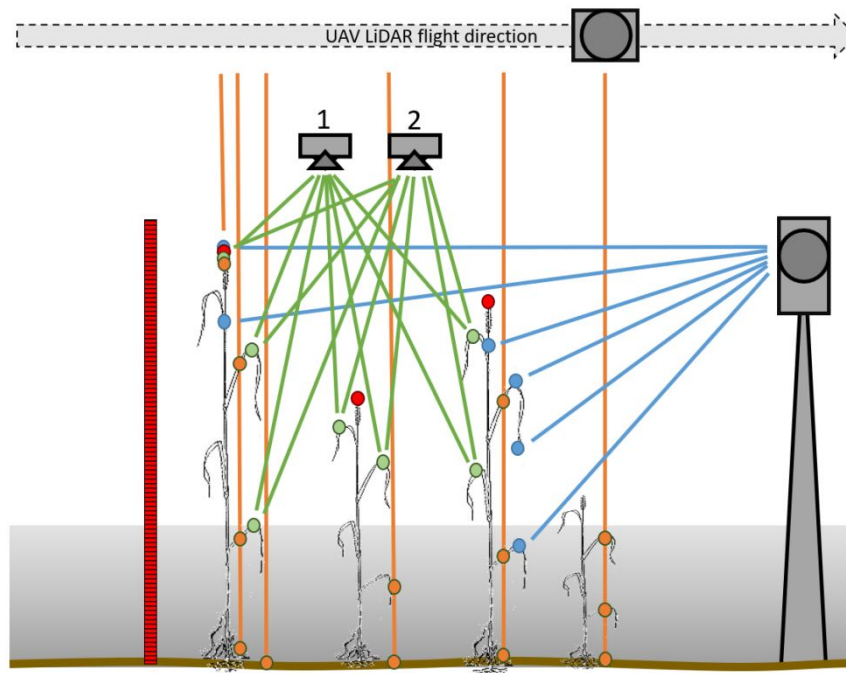
197 Counting approaches overcome the limitations of coverage-based approaches by identifying and
198 counting visible plant organs such as, e.g., leaves. Consequently, those approaches require ground
199 sampling distances that allow to clearly separate tiny plant organs in early growth stages from the soil
200 and from each other. For wheat, this typically demands for ground sampling distances < 0.5 mm per
201 pixel (Roth et al., 2020). With such data, both hand-crafted feature extraction as well as machine
202 learning approaches proved to be useful to estimate plant densities (Liu et al., 2017, 2018).
203 Transferred to UAV data, those approaches require collecting images while flying at very low heights
204 (Jin et al., 2017), which significantly decreases their suitability in large breeding experiments.

205 **3.3. Plant height, growth and lodging**

206 Plant height has become a standard trait to be extracted by UAV remote sensing. In 2010, Hoffmeister
207 et al. (2010) introduced the concept of crop surface models (CSMs) that was later refined by Tilly et al.
208 (2014) to track plant growth and adapted to UAV remote sensing by Bendig et al. (2015, 2014, 2013).
209 With plant height also lodging – as a depression in plant height – can be detected. Plant growth
210 information can then be used to e.g. investigate the interaction of environmental variables, genetic
211 information and stem elongation (Kronenberg et al., 2021, 2017).

212 For UAV sensing systems, laser scanning and image-based approaches are available to extract plant
213 height. Practically, image-based approaches have become most popular since they require cheaper
214 and lighter equipment. With photogrammetric algorithms overlapping 2D images can be aligned and
215 the 3D geometry of an object can be reconstructed using the mathematical model of central projection
216 imaging (Luhmann et al., 2014). Particularly important for UAV remote sensing was the development
217 of the Structure from Motion (SfM) technique within the field of computer vision and its combination
218 with digital photogrammetry (Colomina and Molina, 2014; Eltner and Schneider, 2015). Advances of
219 the latter in image matching (Gruen, 2012), orientation (Remondino et al., 2012) and the process of
220 dense 3D point cloud generation allow the reconstruction of surfaces in very high resolution (Haala,
221 2013).

222 The drawback of SfM is that in contrast to active remote sensing systems such as laser scanners only
223 points visible in at least two images can be reconstructed (Figure 4). Practically, SfM thus can barely
224 penetrate the canopy (Harwin and Lucieer, 2012). Since the structural traits gain increasing attention,
225 UAV laser scanning based approaches hold great potential for field phenotyping applications.



226

227 *Figure 4 Schematics of plant height estimated with a ruler (red), terrestrial laser scanner (blue), UAV*
 228 *(multi-return) laser scanning moving across the area (orange) and structure from motion with two*
 229 *camera positions (green). The active laser scanning systems can penetrate the shade (grey area) (figure*
 230 *adapted from Aasen, 2016).*

231 With the availability of 2D spectral images, spectral and 3D data could be captured at the same time
 232 (Aasen et al., 2015).

233 3.4. Biomass

234 Biomass can be estimated based on structural and spectral approaches. Structural approaches are
 235 mainly based on empirical relationships of biomass and plant height. It has shown great potential to
 236 estimate biomass increase of crops throughout the season (Aasen and Bareth, 2018; Bendig et al.,
 237 2015; Tilly et al., 2015). Still, seen from a theoretical perspective, one can be skeptical when it comes
 238 to the robustness of this approach across genotypes and seasons since the relationship of height to
 239 biomass may vary between genotypes and due to environmental influences. Extracting the mean plant
 240 height per plot represents a massive reduction in dimensionality if working with 3D point clouds as
 241 source. Approaches that include other canopy-related information, e.g., canopy roughness (Herrero-
 242 Huerta et al., 2020), may lead to improved biomass estimations based on structural data.

243 Biomass estimation based on spectral data is very common in remote sensing and is now also
 244 frequently applied in field phenotyping applications. Mostly, empirical relationships are established
 245 between the absorption of an area covered by plants – often measured by means of vegetation indices
 246 – and biomass (Aasen et al., 2014; Bendig et al., 2015; Erdle et al., 2013; Fu et al., 2014; Gnyp, Martin
 247 Leon et al., 2014; Hansen and Schjoerring, 2003; Prabhakara et al., 2015; Tilly et al., 2015). Light
 248 absorption is closely related to the amount of absorbing plant matter (c.f. subsection 3.1.2) and thus,

249 this approach is also from a theoretical point of few more robust than the relationship of plant height
250 to biomass. Still, similar as with LAI, the retrieval of biomass based on empirical relationships with
251 spectral data may not be robust across genotypes, phenological stages and years – and similar to LAI
252 also here inversion of physiological based radiative transfer models in combination with non-
253 parametric machine learning may be a way forward (c.f. subsection 3.1.2).

254 3.5. Flowering and fruiting and yield estimation

255 Flowering and fruiting can be easy to detect for some crops – such as flowering in rapeseed- or very
256 challenging as in the case of flowering in wheat. Overall, two approaches can be used to determine
257 flowering and fruiting. An indirect method is to monitor the change in colorization of the canopy that
258 indicates that reproduction organs are appearing. A direct approach is to directly detect these organs
259 with image processing techniques. Several attempts have been published in this regard that use
260 traditional, handcrafted features (Guo et al., 2015). With the advent of deep learning, this approach
261 has been largely automated. Today convolutional neural networks can be used to segment plants from
262 soil even in challenging conditions (Zenkl et al., “in review”), detect and even count flower heads
263 (Gallmann et al., “in review”) and wheat ears (David et al., 2020). The publications by David et al. (2021,
264 2020) are particularly interesting, since they represent a worldwide effort by many institutions to
265 compile a dataset called the “*Global Wheat Head Dataset*” that now serves as a benchmark dataset
266 for the global machine learning community.

267 Still, for the direct detection approach the ground sampling distance needs to be appropriate which
268 may bring down the throughput due to the necessity to lower the flight altitude in order to achieve
269 the necessary resolution. Luckily, camera technology is developing fast and current very-high
270 resolution camera systems with 100 megapixels are able to ease this issue (Lucieer et al., “in
271 preparation”).

272 Besides the detection aspect, differences in flowering between genotypes can happen within only a
273 few days and thus require a very high revisit frequency of the sensing approach. While this might be
274 feasible for permanently manned research stations, for more remote research fields solutions such as
275 PhenoCams might be a more applicable approach (Aasen et al., 2020).

276 3.6. Senescence

277 Senescence is a developmental process which in annual crop plants overlaps with the reproductive
278 phase. Senescence might reduce crop yield when it is induced prematurely under adverse
279 environmental conditions. On the other hand, a number of studies found that for so-called “stay-
280 green” phenotypes, some are functional stay-green plants with increased productivity due to
281 prolonged carbon assimilation (Gregersen et al., 2013).

282 Since the process of senescence is related with the decolorization of leaf tissue, traditional it is rated
283 as the ratio of decolorized of individual leaves (e.g. flag leaf in wheat) or the whole canopy (Pask et al.,
284 2012). Consequently, also digital methods follow that approach and quantify canopy color. Burkart et
285 al. (Burkart et al., 2018) used the green-red vegetation index to extract canopy greenness from UAV
286 RGB images across two vegetation periods and could identify different growth stages, including
287 ripening / senescence. Other approaches build on spectral data (Anderegg et al., 2020) and may be
288 transferred to flying platforms.

289 **3.7. Canopy temperature**

290 Plants interact with the surrounding environment through carbon, water- and energy-exchange
291 processes, maintaining an equilibrium that permits them to grow and adapt to variable growing
292 conditions. Due to the transpiration cooling effect of water leaving the stomata, this energy exchange,
293 among other processes, affects the temperature of foliage. Based on this relationship, many
294 researchers have taken canopy temperature as proxy for the water status of plants and associated
295 traits, e.g. yield (Li et al., 2019; Lopes and Reynolds, 2010; Rebetzke et al., 2013; Reynolds et al., 1994).

296 Since field measurements are time consuming and often result in low repeatability if environmental
297 conditions change during the measurement (Deery et al., 2016b), airborne thermography (including
298 with UAVs) has gained in popularity. It allows the assessment of canopy temperature in large breeding
299 or genetic experiments in a short time, increasing repeatability as compared to manual plot-by-plot
300 measurements (Deery et al., 2019, 2016a; Gago et al., 2015; Liebisch et al., 2015; Perich et al., 2020).

301 However, the relationship between transpiration and canopy temperature is very complex since it
302 depends on the (micro-) environmental conditions around the plant, e.g. ambient temperature, wind
303 and vapour pressure (Costa et al., 2013; Maes and Steppe, 2012). This poses significant challenges to
304 translate measurements of canopy temperature to physiological meaningful quantities – in particular
305 in areas with potentially fluctuating environmental conditions (such as Switzerland). Several
306 approaches to normalizing this effect and establishing a relationship between canopy temperature and
307 transpiration have been proposed. Experimental approaches include wet and dry reference surfaces
308 into the image, which is challenging to be achieved in UAV remote sensing (Jones, 1999; Maes and
309 Steppe, 2012). Other approaches normalize canopy temperature with air temperature or model
310 reference values based on meteorological data (Berni et al., 2009, 2009; Idso et al., 1981; Jackson et
311 al., 1981; Maes and Steppe, 2012; Zarco-Tejada et al., 2018, 2013). While these existing approaches
312 have been shown to work with airborne and UAV observations in arid and semi-arid regions, to the
313 authors knowledge they have not been validated for crop genotype screening in temperate climates.

314 Further, in cases where the canopy is not fully closed (e.g. wheat), most often a pixel does not contain
315 a pure signal from the foliage, but rather an integrated signal from both soil and vegetation, when the

316 canopy is measured by a UAV sensor at a right angle to that surface (NADIR). Thus, the soil background
317 confounds the signal from the foliage (Deery and Jones, 2021). The degree to which it does so depends
318 on shoot biomass, phenology, morphology and structural parameters of the canopy, such as plant
319 height, leaf area index, ground cover and leaf and spike orientation (reviewed by (Prashar and Jones,
320 2014)). A study by Hund et al. (“in-preparation”) showed that in breeding experiments, where
321 genotypes with different heights are placed next to each other, canopy height is the most important
322 driver for canopy temperature. This finding has great implications for thermal field-phenotyping and
323 in such settings the interpretation of canopy temperature should be handled with care until this effect
324 can be normalized by means of statistical approaches or experimental designs.

325 **4. Conclusion and outlook**

326 The adaption of remote sensing tools by plant scientists has opened new perspectives and provided
327 the base for high-throughput field phenotyping. Today, some remote sensing technology, method or
328 philosophy is part of almost any field phenotyping – may it be by applying proximal handheld, robotic
329 or flying platforms (or a combination of those (Pretto et al., 2021)) or the adaption of sophisticated
330 machine learning approaches to make sense of the big data that results from applying remote sensing
331 systems.

332 However, the rapid adaption of these tools needs to be followed by a deeper understand of the data
333 captured and the information gathered to be able to truly interpret the information carried within the
334 extracted traits. With this text we reviewed recent trends in high-throughput field phenotyping from
335 the perspective of remote sensing – and by that not only highlighted the promising approaches but
336 also gave some background from the remote sensing theory to casting light into the shadows that hide
337 potential pitfalls.

338 But we should not stop here. The remote sensing community is increasing getting aware off the needs
339 of plant scientists and more and more remote sensing researchers are discovering the plant to plot
340 scale as a fruitful field (Machwitz et al., “accepted”). Fostering this development and bringing plant
341 scientist, remote sensing specialist, ecologist, and breeders to the same (dinner) table to exchange
342 ideas and initiate collaborations would allow to unlock the full potential of current remote sensing
343 technologies by faster identifying intersections and enabling the transfer of knowledge. Moreover, this
344 would also allow transferring the insights gained by applying remote sensing technology to the plant
345 to plot scale back to the landscape scale by improving satellite remote sensing approaches. Finally, in
346 the whole field phenotyping community, there is a risk that research is driven by technology rather
347 than applications. Thus, this exchange should go in both ways and we call for plant scientist to help
348 guiding the research activities of remote sensing specialists and the whole field phenotyping
349 community into directions that yield improvements towards a more sustainable agriculture.

350 **5. Authors contribution**

351 H.A. conceived and wrote major parts of the text. L.R.: contributed partially to the text, revised the
352 text, and created Figure 3.

353 **6. Acknowledgements**

354 We acknowledge Quirina Merz for providing the Orthomosaic of the fixed-wing UAV in Figure 2. We
355 acknowledge the funding of the Swiss Science Foundation for the projects “PhenomEn” (grant number
356 IZCOZO_198091), “PhotoInd” (grant number CRSK-3_195591) and “Trait spotting” (grant number KTI
357 P-Nr 27059.2 PFLS-LS) and the Swiss National Science Foundation (SNSF), within the framework of the
358 National Research Programme “Sustainable Economy: resource-friendly, future-oriented, innovative”
359 (NRP 73), in the InnoFarm project, Grant-N° 407340_172433. Also, we thank Radek Zenkl for his
360 contributions to Figure 2 and the whole Crop Science Group of ETH Zürich with Professor Achim Walter
361 and the Remote Sensing and GIS Group at the University of Cologne with Professor Georg Bareth
362 without whom this research would not have been possible.

363 **7. Literature**

- 364 Aasen, H., 2016. The acquisition of hyperspectral digital surface models of crops from UAV snapshot
365 cameras (Dissertation). University of Cologne, Cologne, Germany.
- 366 Aasen, H., Bareth, G., 2018. Ground and UAV sensing approaches for spectral and 3D crop trait
367 estimation, in: Thenkabail, P., Lyon, J.G., Huete, A. (Eds.), *Hyperspectral Remote Sensing of*
368 *Vegetation - Volume II: Biophysical and Biochemical Characterization and Plant Species*
369 *Studies*. Chapman and Hall/CRC, Milton.
- 370 Aasen, H., Burkart, A., Bolten, A., Bareth, G., 2015. Generating 3D hyperspectral information with
371 lightweight UAV snapshot cameras for vegetation monitoring: From camera calibration to
372 quality assurance. *ISPRS J. Photogramm. Remote Sens.* 108, 245–259.
373 <https://doi.org/10.1016/j.isprsjprs.2015.08.002>
- 374 Aasen, H., Gnyp, M.L., Miao, Y., Bareth, G., 2014. Automated Hyperspectral Vegetation Index Retrieval
375 from Multiple Correlation Matrices with HyperCor. *Photogramm. Eng. Remote Sens.* 80, 785–
376 795. <https://doi.org/10.14358/PERS.80.8.785>
- 377 Aasen, H., Honkavaara, E., Lucieer, A., Zarco-Tejada, P., 2018. Quantitative Remote Sensing at Ultra-
378 High Resolution with UAV Spectroscopy: A Review of Sensor Technology, Measurement
379 Procedures, and Data Correction Workflows. *Remote Sens.* 10, 1091.
380 <https://doi.org/10.3390/rs10071091>
- 381 Aasen, H., Kirchgessner, N., Walter, A., Liebisch, F., 2020. PhenoCams for Field Phenotyping: Using Very
382 High Temporal Resolution Digital Repeated Photography to Investigate Interactions of Growth,
383 Phenology, and Harvest Traits. *Front. Plant Sci.* 11, 593.
384 <https://doi.org/10.3389/fpls.2020.00593>
- 385 Adão, T., Hruška, J., Pádua, L., Bessa, J., Peres, E., Morais, R., Sousa, J., 2017. Hyperspectral Imaging: A
386 Review on UAV-Based Sensors, Data Processing and Applications for Agriculture and Forestry.
387 *Remote Sens.* 9, 1110. <https://doi.org/10.3390/rs9111110>
- 388 Anderegg, J., Yu, K., Aasen, H., Walter, A., Liebisch, F., Hund, A., 2020. Spectral Vegetation Indices to
389 Track Senescence Dynamics in Diverse Wheat Germplasm. *Front. Plant Sci.* 10, 1749.
390 <https://doi.org/10.3389/fpls.2019.01749>
- 391 Anderson, K., Gaston, K.J., 2013. Lightweight unmanned aerial vehicles will revolutionize spatial
392 ecology. *Front. Ecol. Environ.* 11, 138–146. <https://doi.org/10.1890/120150>

393 Araus, J.L., Cairns, J.E., 2014. Field high-throughput phenotyping: the new crop breeding frontier.
394 Trends Plant Sci. 19, 52–61. <https://doi.org/10.1016/j.tplants.2013.09.008>

395 Araus, J.L., Kefauver, S.C., Zaman-Allah, M., Olsen, M.S., Cairns, J.E., 2018. Translating High-Throughput
396 Phenotyping into Genetic Gain. Trends Plant Sci. 23, 451–466.
397 <https://doi.org/10.1016/j.tplants.2018.02.001>

398 Atzberger, C., Guérif, M., Baret, F., Werner, W., 2010. Comparative analysis of three chemometric
399 techniques for the spectroradiometric assessment of canopy chlorophyll content in winter
400 wheat. Comput. Electron. Agric. 73, 165–173. <https://doi.org/10.1016/j.compag.2010.05.006>

401 Bendig, J., Bolten, A., Bareth, G., 2013. UAV-based Imaging for Multi-Temporal, very high Resolution
402 Crop Surface Models to monitor Crop Growth Variability. Photogramm. - Fernerkund. -
403 Geoinformation 2013, 551–562. <https://doi.org/10.1127/1432-8364/2013/0200>

404 Bendig, J., Bolten, A., Bennertz, S., Broscheit, J., Eichfuss, S., Bareth, G., 2014. Estimating Biomass of
405 Barley Using Crop Surface Models (CSMs) Derived from UAV-Based RGB Imaging. Remote Sens.
406 6, 10395–10412. <https://doi.org/10.3390/rs61110395>

407 Bendig, J., Yu, K., Aasen, H., Bolten, A., Bennertz, S., Broscheit, J., Gnyp, M.L., Bareth, G., 2015.
408 Combining UAV-based plant height from crop surface models, visible, and near infrared
409 vegetation indices for biomass monitoring in barley. Int. J. Appl. Earth Obs. Geoinformation
410 39, 79–87. <https://doi.org/10.1016/j.jag.2015.02.012>

411 Berni, J.A.J., Zarco-Tejada, P.J., Sepulcre-Cantó, G., Fereres, E., Villalobos, F., 2009. Mapping canopy
412 conductance and CWSI in olive orchards using high resolution thermal remote sensing
413 imagery. Remote Sens. Environ. 113, 2380–2388. <https://doi.org/10.1016/j.rse.2009.06.018>

414 Burkart, A., Hecht, V.L., Kraska, T., Rascher, U., 2018. Phenological analysis of unmanned aerial vehicle
415 based time series of barley imagery with high temporal resolution. Precis. Agric. 19, 134–146.
416 <https://doi.org/10.1007/s11119-017-9504-y>

417 Cendrero-Mateo, M.P., Muller, O., Albrecht, H., Burkart, A., Gatzke, S., Janssen, B., Keller, B., Körber,
418 N., Kraska, T., Matsubara, S., Jinquan, L., Müller-Linow, M., Pieruschka, R., Pinto, F., Rischbeck,
419 P., Schickling, A., Steier, A., Watt, M., Schurr, U., Rascher, U., 2017. Field phenotyping: concepts
420 and examples to quantify dynamic plant traits across scales in the field, in: Chabbi, A.,
421 Loescher, H.W. (Eds.), Terrestrial Ecosystem Research Infrastructures: Challenges and
422 Opportunities, Abad Chabbi, Abad Chabbi, Henry W. Loescher; CRC Press, Boca Raton, pp. 53–
423 80.

424 Colomina, I., Molina, P., 2014. Unmanned aerial systems for photogrammetry and remote sensing: A
425 review. ISPRS J. Photogramm. Remote Sens. 92, 79–97.
426 <https://doi.org/10.1016/j.isprsjprs.2014.02.013>

427 Costa, J.M., Grant, O.M., Chaves, M.M., 2013. Thermography to explore plant-environment
428 interactions. J. Exp. Bot. 64, 3937–3949. <https://doi.org/10.1093/jxb/ert029>

429 David, E., Madec, S., Sadeghi-Tehran, P., Aasen, H., Zheng, B., Liu, S., Kirchgessner, N., Ishikawa, G.,
430 Nagasawa, K., Badhon, M.A., Pozniak, C., de Solan, B., Hund, A., Chapman, S.C., Baret, F.,
431 Stavness, I., Guo, W., 2020. Global Wheat Head Detection (GWHD) Dataset: A Large and
432 Diverse Dataset of High-Resolution RGB-Labelled Images to Develop and Benchmark Wheat
433 Head Detection Methods. Plant Phenomics 2020, 1–12.
434 <https://doi.org/10.34133/2020/3521852>

435 David, E., Serouart, M., Smith, D., Madec, S., Velumani, K., Liu, S., Wang, X., Espinosa, F.P., Shafiee, S.,
436 Tahir, I.S.A., Tsujimoto, H., Nasuda, S., Zheng, B., Kirchgessner, N., Aasen, H., Hund, A., Sadhegi-
437 Tehran, P., Nagasawa, K., Ishikawa, G., Dandri-fosse, S., Carlier, A., Mercatoris, B., Kuroki, K.,
438 Wang, H., Ishii, M., Badhon, M.A., Pozniak, C., LeBauer, D.S., Lilimo, M., Poland, J., Chapman,
439 S., de Solan, B., Baret, F., Stavness, I., Guo, W., 2021. Global Wheat Head Dataset 2021: more
440 diversity to improve the benchmarking of wheat head localization methods. ArXiv210507660
441 Cs.

442 Deery, D.M., Jones, H.G., 2021. Field Phenomics: Will It Enable Crop Improvement? Plant Phenomics
443 2021, 1–16. <https://doi.org/10.34133/2021/9871989>

444 Deery, D.M., Rebetzke, G.J., Jimenez-Berni, J.A., Bovill, W.D., James, R.A., Condon, A.G., Furbank, R.T.,
445 Chapman, S.C., Fischer, R.A., 2019. Evaluation of the Phenotypic Repeatability of Canopy

446 Temperature in Wheat Using Continuous-Terrestrial and Airborne Measurements. *Front. Plant*
447 *Sci.* 10, 875. <https://doi.org/10.3389/fpls.2019.00875>

448 Deery, D.M., Rebetzke, G.J., Jimenez-Berni, J.A., James, R.A., Condon, A.G., Bovill, W.D., Hutchinson,
449 P., Scarrow, J., Davy, R., Furbank, R.T., 2016a. Methodology for High-Throughput Field
450 Phenotyping of Canopy Temperature Using Airborne Thermography. *Front. Plant Sci.* 7.
451 <https://doi.org/10.3389/fpls.2016.01808>

452 Deery, D.M., Rebetzke, G.J., Jimenez-Berni, J.A., James, R.A., Condon, A.G., Bovill, W.D., Hutchinson,
453 P., Scarrow, J., Davy, R., Furbank, R.T., 2016b. Methodology for High-Throughput Field
454 Phenotyping of Canopy Temperature Using Airborne Thermography. *Front. Plant Sci.* 7.
455 <https://doi.org/10.3389/fpls.2016.01808>

456 Eltner, A., Schneider, D., 2015. Analysis of Different Methods for 3D Reconstruction of Natural Surfaces
457 from Parallel-Axes UAV Images. *Photogramm. Rec.* 30, 279–299.
458 <https://doi.org/10.1111/phor.12115>

459 Erdle, K., Mistele, B., Schmidhalter, U., 2013. Spectral high-throughput assessments of phenotypic
460 differences in biomass and nitrogen partitioning during grain filling of wheat under high
461 yielding Western European conditions. *Field Crops Res.* 141, 16–26.
462 <https://doi.org/10.1016/j.fcr.2012.10.018>

463 Fu, Y., Yang, G., Wang, J., Song, X., Feng, H., 2014. Winter wheat biomass estimation based on spectral
464 indices, band depth analysis and partial least squares regression using hyperspectral
465 measurements. *Comput. Electron. Agric.* 100, 51–59.
466 <https://doi.org/10.1016/j.compag.2013.10.010>

467 Furbank, R.T., Tester, M., 2011. Phenomics – technologies to relieve the phenotyping bottleneck.
468 *Trends Plant Sci.* 16, 635–644. <https://doi.org/10.1016/j.tplants.2011.09.005>

469 Gago, J., Douthe, C., Coopman, R.E., Gallego, P.P., Ribas-Carbo, M., Flexas, J., Escalona, J., Medrano,
470 H., 2015. UAVs challenge to assess water stress for sustainable agriculture. *Agric. Water*
471 *Manag.* 153, 9–19. <https://doi.org/10.1016/j.agwat.2015.01.020>

472 Gallmann, J., Schüpbach, B., Jacot, K., Albrecht, M., Winizki, J., Aasen, H., “in review.” Flower Mapping
473 in Grasslands with Drones and Deep Learning.

474 Gnyp, Martin Leon, Miao, Yuxin, Yuan, Fei, Yu, Kang, Yao, Yinkun, Huang, S., Bareth, Georg, 2014.
475 Derivative analysis to improve rice biomass estimation at early growth stages.
476 <https://doi.org/10.5880/TR32DB.KGA94.7>

477 Gnyp, M.L., Yu, K., Aasen, H., Yao, Y., Huang, S., Miao, Y., Bareth, G., 2013. Analysis of Crop Reflectance
478 for Estimating Biomass in Rice Canopies at Different Phenological Stages. *Photogramm. -*
479 *Fernerkund. - Geoinformation* 2013, 351–365. <https://doi.org/10.1127/1432-8364/2013/0182>

480 Gregersen, P.L., Culetic, A., Boschian, L., Krupinska, K., 2013. Plant senescence and crop productivity.
481 *Plant Mol. Biol.* 82, 603–622. <https://doi.org/10.1007/s11103-013-0013-8>

482 Gruen, A., 2012. Development and Status of Image Matching in Photogrammetry: Development and
483 status of image matching in photogrammetry. *Photogramm. Rec.* 27, 36–57.
484 <https://doi.org/10.1111/j.1477-9730.2011.00671.x>

485 Guo, W., Fukatsu, T., Ninomiya, S., 2015. Automated characterization of flowering dynamics in rice
486 using field-acquired time-series RGB images. *Plant Methods* 11, 7.
487 <https://doi.org/10.1186/s13007-015-0047-9>

488 Haala, N., 2013. The Landscape of Dense Image Matching Algorithms. Presented at the
489 Photogrammetric Week'13, pp. 271–284.

490 Hansen, P.M., Schjoerring, J.K., 2003. Reflectance measurement of canopy biomass and nitrogen status
491 in wheat crops using normalized difference vegetation indices and partial least squares
492 regression. *Remote Sens. Environ.* 86, 542–553. [https://doi.org/10.1016/S0034-4257\(03\)00131-7](https://doi.org/10.1016/S0034-4257(03)00131-7)

493
494 Harwin, S., Lucieer, A., 2012. Assessing the Accuracy of Georeferenced Point Clouds Produced via
495 Multi-View Stereopsis from Unmanned Aerial Vehicle (UAV) Imagery. *Remote Sens.* 4, 1573–
496 1599. <https://doi.org/10.3390/rs4061573>

497 Herrero-Huerta, M., Bucksch, A., Puttonen, E., Rainey, K.M., 2020. Canopy Roughness: A New
498 Phenotypic Trait to Estimate Aboveground Biomass from Unmanned Aerial System. *Plant*
499 *Phenomics* 2020, 1–10. <https://doi.org/10.34133/2020/6735967>

500 Hoffmeister, D., Bolten, A., Curdt, C., Waldhoff, G., Bareth, G., 2010. High-resolution Crop Surface
501 Models (CSM) and Crop Volume Models (CVM) on field level by terrestrial laser scanning, in:
502 *The Sixth International Symposium on Digital Earth*. International Society for Optics and
503 Photonics, p. 6.

504 Hu, P., Guo, W., Chapman, S.C., Guo, Y., Zheng, B., 2019. Pixel size of aerial imagery constrains the
505 applications of unmanned aerial vehicle in crop breeding. *ISPRS J. Photogramm. Remote Sens.*
506 154, 1–9. <https://doi.org/10.1016/j.isprsjprs.2019.05.008>

507 Hund, A., Kislinger, F., Aasen, H., “in-preparation.” Plant height drives canopy temperature in breeding
508 experiments.

509 Hund, A., Kronenberg, L., Anderegg, J., Yu, K., Walter, A., 2019a. Non-invasive phenotyping of cereal
510 growth and development characteristics in the field, in: Ordon, F., Friedt, W. (Eds.), *Advances*
511 *in Crop Breeding Techniques*. Burleigh Dodds.

512 Hund, A., Kronenberg, L., Anderegg, J., Yu, K., Walter, A., 2019b. Non-invasive field phenotyping of
513 cereal development 249–292. <https://doi.org/10.19103/as.2019.0051.13>

514 Idso, S.B., Jackson, R.D., Pinter, P.J., Reginato, R.J., Hatfield, J.L., 1981. Normalizing the stress-degree-
515 day parameter for environmental variability. *Agric. Meteorol.* 24, 45–55.
516 [https://doi.org/10.1016/0002-1571\(81\)90032-7](https://doi.org/10.1016/0002-1571(81)90032-7)

517 Jackson, R.D., Idso, S.B., Reginato, R.J., Pinter, P.J., 1981. Canopy temperature as a crop water stress
518 indicator. *Water Resour. Res.* 17, 1133–1138. <https://doi.org/10.1029/WR017i004p01133>

519 Jin, X., Liu, S., Baret, F., Hemerlé, M., Comar, A., 2017. Estimates of plant density of wheat crops at
520 emergence from very low altitude UAV imagery. *Remote Sens. Environ.* 198, 105–114.
521 <https://doi.org/10.1016/j.rse.2017.06.007>

522 Jones, H.G., 1999. Use of thermography for quantitative studies of spatial and temporal variation of
523 stomatal conductance over leaf surfaces. *Plant Cell Environ.* 22, 1043–1055.
524 <https://doi.org/10.1046/j.1365-3040.1999.00468.x>

525 Kirchgessner, N., Liebisch, F., Yu, K., Pfeifer, J., Friedli, M., Hund, A., Walter, A., 2017. The ETH field
526 phenotyping platform FIP: A cable-suspended multi-sensor system. *Funct. Plant Biol.* 44, 154–
527 168. <https://doi.org/10.1071/FP16165>

528 Kronenberg, L., Yates, S., Boer, M.P., Kirchgessner, N., Walter, A., Hund, A., 2021. Temperature
529 response of wheat affects final height and the timing of stem elongation under field conditions.
530 *J. Exp. Bot.* 72, 700–717. <https://doi.org/10.1093/jxb/eraa471>

531 Kronenberg, L., Yu, K., Walter, A., Hund, A., 2017. Monitoring the dynamics of wheat stem elongation:
532 genotypes differ at critical stages. *Euphytica* 213. <https://doi.org/10.1007/s10681-017-1940-2>

533 Li, X., Ingvordsen, C.H., Weiss, M., Rebetzke, G.J., Condon, A.G., James, R.A., Richards, R.A., 2019.
534 Deeper roots associated with cooler canopies, higher normalized difference vegetation index,
535 and greater yield in three wheat populations grown on stored soil water. *J. Exp. Bot.* 70, 4963–
536 4974. <https://doi.org/10.1093/jxb/erz232>

537 Liebisch, F., Kirchgessner, N., Schneider, D., Walter, A., Hund, A., 2015. Remote, aerial phenotyping of
538 maize traits with a mobile multi-sensor approach. *Plant Methods* 11, 9.
539 <https://doi.org/10.1186/s13007-015-0048-8>

540 Liu, S., Baret, F., Andrieu, B., Burger, P., Hemmerlé, M., 2017. Estimation of Wheat Plant Density at
541 Early Stages Using High Resolution Imagery. *Front. Plant Sci.* 8, 739.
542 <https://doi.org/10.3389/fpls.2017.00739>

543 Liu, T., Yang, T., Li, C., Li, R., Wu, W., Zhong, X., Sun, C., Guo, W., 2018. A method to calculate the
544 number of wheat seedlings in the 1st to the 3rd leaf growth stages. *Plant Methods* 14, 101.
545 <https://doi.org/10.1186/s13007-018-0369-5>

546 Lopes, M.S., Reynolds, M.P., 2010. Partitioning of assimilates to deeper roots is associated with cooler
547 canopies and increased yield under drought in wheat. *Funct. Plant Biol.* 37, 147.
548 <https://doi.org/10.1071/FP09121>

549 Lucieer, A., ..., Aasen, H., ..., "in preparation." Advances in remote sensing of vegetation with drones –
550 review and outlook.

551 Machwitz, M., Pieruschka, R., Berger, K., Schlerf, M., Aasen, H., Fahrner, S., Jimenez-Berni, J.A., Baret,
552 F., Rascher, U., "accepted." Bridging the gap between remote sensing and plant phenotyping
553 - challenges and opportunities for the next generation of sustainable agriculture. *Front. Plant*
554 *Sci.*

555 Maes, W.H., Steppe, K., 2019. Perspectives for Remote Sensing with Unmanned Aerial Vehicles in
556 Precision Agriculture. *Trends Plant Sci.* 24, 152–164.
557 <https://doi.org/10.1016/j.tplants.2018.11.007>

558 Maes, W.H., Steppe, K., 2012. Estimating evapotranspiration and drought stress with ground-based
559 thermal remote sensing in agriculture: a review. *J. Exp. Bot.* 63, 4671–4712.
560 <https://doi.org/10.1093/jxb/ers165>

561 McCabe, M.F., Rodell, M., Alsdorf, D.E., Miralles, D.G., Uijlenhoet, R., Wagner, W., Lucieer, A., Houborg,
562 R., Verhoest, N.E.C., Franz, T.E., Shi, J., Gao, H., Wood, E.F., 2017. The future of Earth
563 observation in hydrology. *Hydrol. Earth Syst. Sci.* 21, 3879–3914.
564 <https://doi.org/10.5194/hess-21-3879-2017>

565 Pádua, L., Vanko, J., Hruška, J., Adão, T., Sousa, J.J., Peres, E., Morais, R., 2017. UAS, sensors, and data
566 processing in agroforestry: a review towards practical applications. *Int. J. Remote Sens.* 1–43.
567 <https://doi.org/10.1080/01431161.2017.1297548>

568 Pajares, G., 2015. Overview and Current Status of Remote Sensing Applications Based on Unmanned
569 Aerial Vehicles (UAVs). *Photogramm. Eng. Remote Sens.* 81, 281–330.
570 <https://doi.org/10.14358/PERS.81.4.281>

571 Pask, A., Pietragalla, J., Mullan, D., Reynolds, M. (Eds.), 2012. Physiological breeding II : a field guide to
572 wheat phenotyping. CIMMYT, Mexico.

573 Perich, G., Hund, A., Anderegg, J., Roth, L., Boer, M.P., Walter, A., Liebisch, F., Aasen, H., 2020.
574 Assessment of Multi-Image Unmanned Aerial Vehicle Based High-Throughput Field
575 Phenotyping of Canopy Temperature. *Front. Plant Sci.* 11, 150.
576 <https://doi.org/10.3389/fpls.2020.00150>

577 Phillips, S.B., Keahey, D.A., Warren, J.G., Mullins, G.L., 2004. Estimating Winter Wheat Tiller Density
578 Using Spectral Reflectance Sensors for Early-Spring, Variable-Rate Nitrogen Applications.
579 *Agron. J.* 96, 1. <https://doi.org/10.2134/agronj2004.0591>

580 Prabhakara, K., Hively, W.D., McCarty, G.W., 2015. Evaluating the relationship between biomass,
581 percent groundcover and remote sensing indices across six winter cover crop fields in
582 Maryland, United States. *Int. J. Appl. Earth Obs. Geoinformation* 39, 88–102.
583 <https://doi.org/10.1016/j.jag.2015.03.002>

584 Prashar, A., Jones, H., 2014. Infra-Red Thermography as a High-Throughput Tool for Field Phenotyping.
585 *Agronomy* 4, 397–417. <https://doi.org/10.3390/agronomy4030397>

586 Pretto, A., Aravecchia, S., Burgard, W., Chebrolu, N., Dornhege, C., Falck, T., Fleckenstein, F.V.,
587 Fontenla, A., Imperoli, M., Khanna, R., Liebisch, F., Lottes, P., Milioto, A., Nardi, D., Nardi, S.,
588 Pfeifer, J., Popovic, M., Potena, C., Pradalier, C., Rothacker-Feder, E., Sa, I., Schaefer, A.,
589 Siegwart, R., Stachniss, C., Walter, A., Winterhalter, W., Wu, X., Nieto, J., 2021. Building an
590 Aerial–Ground Robotics System for Precision Farming: An Adaptable Solution. *IEEE Robot.*
591 *Autom. Mag.* 28, 29–49. <https://doi.org/10.1109/MRA.2020.3012492>

592 Rasmussen, J., Ntakos, G., Nielsen, J., Svensgaard, J., Poulsen, R.N., Christensen, S., 2016. Are
593 vegetation indices derived from consumer-grade cameras mounted on UAVs sufficiently
594 reliable for assessing experimental plots? *Eur. J. Agron.* 74, 75–92.
595 <https://doi.org/10.1016/j.eja.2015.11.026>

596 Rebetzke, G.J., Jimenez-Berni, J., Fischer, R.A., Deery, D.M., Smith, D.J., 2019. Review: High-throughput
597 phenotyping to enhance the use of crop genetic resources. *Plant Sci.* 282, 40–48.
598 <https://doi.org/10.1016/j.plantsci.2018.06.017>

599 Rebetzke, G.J., Rattey, A.R., Farquhar, G.D., Richards, R.A., Condon, A.T.G., 2013. Genomic regions for
600 canopy temperature and their genetic association with stomatal conductance and grain yield
601 in wheat. *Funct. Plant Biol.* 40, 14–33. <https://doi.org/10.1071/FP12184>

602 Remondino, F., Del Pizzo, S., Kersten, T.P., Troisi, S., 2012. Low-Cost and Open-Source Solutions for
603 Automated Image Orientation – A Critical Overview, in: Ioannides, M., Fritsch, D., Leissner, J.,
604 Davies, R., Remondino, F., Caffo, R. (Eds.), *Progress in Cultural Heritage Preservation*. Springer
605 Berlin Heidelberg, Berlin, Heidelberg, pp. 40–54.

606 Reynolds, M., Balota, M., Delgado, M., Amani, I., Fischer, R., 1994. Physiological and Morphological
607 Traits Associated With Spring Wheat Yield Under Hot, Irrigated Conditions. *Funct. Plant Biol.*
608 21, 717. <https://doi.org/10.1071/PP9940717>

609 Roth, L., Aasen, H., Walter, A., Liebisch, F., 2018a. Extracting leaf area index using viewing geometry
610 effects—A new perspective on high-resolution unmanned aerial system photography. *ISPRS J.*
611 *Photogramm. Remote Sens.* 141, 161–175. <https://doi.org/10.1016/j.isprsjsprs.2018.04.012>

612 Roth, L., Camenzind, M., Aasen, H., Kronenberg, L., Barendregt, C., Camp, K.-H., Walter, A.,
613 Kirchgessner, N., Hund, A., 2020. Repeated Multiview Imaging for Estimating Seedling Tiller
614 Counts of Wheat Genotypes Using Drones. *Plant Phenomics* 2020, 1–20.
615 <https://doi.org/10.34133/2020/3729715>

616 Roth, L., Hund, A., Aasen, H., 2018b. PhenoFly Planning Tool: flight planning for high-resolution optical
617 remote sensing with unmanned areal systems. *Plant Methods* 14.
618 <https://doi.org/10.1186/s13007-018-0376-6>

619 Rouse, Jr., J.W., Haas, R.H., Schell, J.A., Deering, D.W., 1974. Monitoring Vegetation Systems in the
620 Great Plains with ERTS, in: *Third Earth Resources Technology Satellite-1 Symposium- Volume I:*
621 *Technical Presentations*. NASA, Washington, D.C., pp. 309–317.

622 Sagan, V., Maimaitijiang, M., Sidike, P., Eblimit, K., Peterson, K.T., Hartling, S., Esposito, F., Khanal, K.,
623 Newcomb, M., Pauli, D., Ward, R., Fritschi, F., Shakoor, N., Mockler, T., 2019. UAV-based high
624 resolution thermal imaging for vegetation monitoring, and plant phenotyping using ICI 8640 P,
625 FLIR Vue Pro R 640, and thermomap cameras. *Remote Sens.* 11.
626 <https://doi.org/10.3390/rs11030330>

627 Sanchez-Azofeifa, A., Antonio Guzmán, J., Campos, C.A., Castro, S., Garcia-Millan, V., Nightingale, J.,
628 Rankine, C., 2017. Twenty-first century remote sensing technologies are revolutionizing the
629 study of tropical forests. *Biotropica* 49, 604–619. <https://doi.org/10.1111/btp.12454>

630 Scotford, I.M., Miller, P.C.H., 2004. Estimating Tiller Density and Leaf Area Index of Winter Wheat using
631 Spectral Reflectance and Ultrasonic Sensing Techniques. *Biosyst. Eng.* 89, 395–408.
632 <https://doi.org/10.1016/j.biosystemseng.2004.08.019>

633 Tardieu, F., Cabrera-Bosquet, L., Pridmore, T., Bennett, M., 2017. Plant Phenomics, From Sensors to
634 Knowledge. *Curr. Biol.* 27, R770–R783. <https://doi.org/10.1016/j.cub.2017.05.055>

635 Tilly, N., Aasen, H., Bareth, G., 2015. Fusion of Plant Height and Vegetation Indices for the Estimation
636 of Barley Biomass. *Remote Sens.* 7, 11449–11480. <https://doi.org/10.3390/rs70911449>

637 Tilly, N., Hoffmeister, D., Cao, Q., Huang, S., Lenz-Wiedemann, V., Miao, Y., Bareth, G., 2014.
638 Multitemporal crop surface models: accurate plant height measurement and biomass
639 estimation with terrestrial laser scanning in paddy rice. *J. Appl. Remote Sens.* 8, 083671.
640 <https://doi.org/10.1117/1.JRS.8.083671>

641 Torres-Sánchez, J., Peña, J.M., de Castro, A.I., López-Granados, F., 2014. Multi-temporal mapping of
642 the vegetation fraction in early-season wheat fields using images from UAV. *Comput. Electron.*
643 *Agric.* 103, 104–113. <https://doi.org/10.1016/j.compag.2014.02.009>

644 Verrelst, J., Camps-Valls, G., Muñoz-Marí, J., Rivera, J.P., Veroustraete, F., Clevers, J.G.P.W., Moreno,
645 J., 2015. Optical remote sensing and the retrieval of terrestrial vegetation bio-geophysical
646 properties – A review. *ISPRS J. Photogramm. Remote Sens.* 108, 273–290.
647 <https://doi.org/10.1016/j.isprsjsprs.2015.05.005>

648 Verrelst, J., Malenovsky, Z., Van der Tol, C., Camps-Valls, G., Gastellu-Etchegorry, J.-P., Lewis, P., North,
649 P., Moreno, J., 2019. Quantifying Vegetation Biophysical Variables from Imaging Spectroscopy
650 Data: A Review on Retrieval Methods. *Surv. Geophys.* 40, 589–629.
651 <https://doi.org/10.1007/s10712-018-9478-y>

652 Virlet, N., Sabermanesh, K., Sadeghi-Tehran, P., Hawkesford, M.J., 2017. Field Scanalyzer: An
653 automated robotic field phenotyping platform for detailed crop monitoring. *Funct. Plant Biol.*
654 44, 143–153. <https://doi.org/10.1071/FP16163>

655 Walter, A., Liebisch, F., Hund, A., 2015. Plant phenotyping: from bean weighing to image analysis. *Plant*
656 *Methods* 11, 14. <https://doi.org/10.1186/s13007-015-0056-8>

657 Wan, L., Zhu, J., Du, X., Zhang, J., Han, X., Zhou, W., Li, X., Liu, J., Liang, F., He, Y., Cen, H., 2021. A model
658 for phenotyping crop fractional vegetation cover using imagery from unmanned aerial
659 vehicles. *J. Exp. Bot.* 72, 4691–4707. <https://doi.org/10.1093/jxb/erab194>

660 Warner, T.A., Cracknell, A.P., 2017. Unmanned aerial vehicles for environmental applications. *Int. J.*
661 *Remote Sens.* 1–8. <https://doi.org/10.1080/01431161.2017.1301705>

662 Yang, G., Liu, J., Zhao, C., Li, Zhenhong, Huang, Y., Yu, H., Xu, B., Yang, X., Zhu, D., Zhang, X., Zhang, R.,
663 Feng, H., Zhao, X., Li, Zhenhai, Li, H., Yang, H., 2017. Unmanned Aerial Vehicle Remote Sensing
664 for Field-Based Crop Phenotyping: Current Status and Perspectives. *Front. Plant Sci.* 8.
665 <https://doi.org/10.3389/fpls.2017.01111>

666 Zarco-Tejada, P.J., 2008. A new era in remote sensing of crops with unmanned robots. *SPIE Newsroom.*
667 <https://doi.org/10.1117/2.1200812.1438>

668 Zarco-Tejada, P.J., Camino, C., Beck, P.S.A., Calderon, R., Hornero, A., Hernández-Clemente, R.,
669 Kattenborn, T., Montes-Borrego, M., Susca, L., Morelli, M., Gonzalez-Dugo, V., North, P.R.J.,
670 Landa, B.B., Boscia, D., Saponari, M., Navas-Cortes, J.A., 2018. Previsual symptoms of *Xylella*
671 *fastidiosa* infection revealed in spectral plant-trait alterations. *Nat. Plants* 4, 432–439.
672 <https://doi.org/10.1038/s41477-018-0189-7>

673 Zarco-Tejada, P.J., González-Dugo, V., Williams, L.E., Suárez, L., Berni, J.A.J., Goldhamer, D., Fereres, E.,
674 2013. A PRI-based water stress index combining structural and chlorophyll effects: Assessment
675 using diurnal narrow-band airborne imagery and the CWSI thermal index. *Remote Sens.*
676 *Environ.* 138, 38–50. <https://doi.org/10.1016/j.rse.2013.07.024>

677 Zenkl, R., Timofte, R., Kirchgessner, N., van Gool, L., Walter, A., Aasen, H., “in review.” *Outdoor Wheat*
678 *Segmentation with Deep Learning.*

679 Zhang, C., Kovacs, J.M., 2012. The application of small unmanned aerial systems for precision
680 agriculture: a review. *Precis. Agric.* 13, 693–712. <https://doi.org/10.1007/s11119-012-9274-5>

681 Zou, X., Haikarainen, Iina, Haikarainen, Iikka, Mäkelä, P., Möttus, M., Pellikka, P., 2018. Effects of Crop
682 Leaf Angle on LAI-Sensitive Narrow-Band Vegetation Indices Derived from Imaging
683 Spectroscopy. *Appl. Sci.* 8, 1435. <https://doi.org/10.3390/app8091435>

684 Zou, X., Möttus, M., 2015. Retrieving crop leaf tilt angle from imaging spectroscopy data. *Agric. For.*
685 *Meteorol.* 205, 73–82. <https://doi.org/10.1016/j.agrformet.2015.02.016>

686